



## ARTICLE

# Minimal contribution of IP<sub>3</sub>R2 in cardiac differentiation and derived ventricular-like myocytes from human embryonic stem cells

Peng Zhang<sup>1,2</sup>, Ji-jun Huang<sup>1</sup>, Kun-fu Ou-yang<sup>3</sup>, He Liang<sup>1</sup>, Miao-ling Li<sup>4</sup>, Yi-jie Wang<sup>1</sup> and Huang-tian Yang<sup>1,2,5</sup>

Type 2 inositol 1,4,5-trisphosphate receptor (IP<sub>3</sub>R2) regulates the intracellular Ca<sup>2+</sup> release from endoplasmic reticulum in human embryonic stem cells (hESCs), cardiovascular progenitor cells (CVPCs), and mammalian cardiomyocytes. However, the role of IP<sub>3</sub>R2 in human cardiac development is unknown and its function in mammalian cardiomyocytes is controversial. hESC-derived cardiomyocytes have unique merits in disease modeling, cell therapy, and drug screening. Therefore, understanding the role of IP<sub>3</sub>R2 in the generation and function of human cardiomyocytes would be valuable for the application of hESC-derived cardiomyocytes. In the current study, we investigated the role of IP<sub>3</sub>R2 in the differentiation of hESCs to cardiomyocytes and in the hESC-derived cardiomyocytes. By using IP<sub>3</sub>R2 knockout (IP<sub>3</sub>R2KO) hESCs, we showed that IP<sub>3</sub>R2KO did not affect the self-renewal of hESCs as well as the differentiation ability of hESCs into CVPCs and cardiomyocytes. Furthermore, we demonstrated the ventricular-like myocyte characteristics of hESC-derived cardiomyocytes. Under the α<sub>1</sub>-adrenergic stimulation by phenylephrine (10 μmol/L), the amplitude and maximum rate of depolarization of action potential (AP) were slightly affected in the IP<sub>3</sub>R2KO hESC-derived cardiomyocytes at differentiation day 90, whereas the other parameters of APs and the Ca<sup>2+</sup> transients did not show significant changes compared with these in the wide-type ones. These results demonstrate that IP<sub>3</sub>R2 has minimal contribution to the differentiation and function of human cardiomyocytes derived from hESCs, thus provide the new knowledge to the function of IP<sub>3</sub>R2 in the generation of human cardiac lineage cells and in the early cardiomyocytes.

**Keywords:** IP<sub>3</sub>R2; human embryonic stem cells; differentiation; cardiovascular progenitor cells; cardiomyocytes; function

*Acta Pharmacologica Sinica* (2020) 41:1576–1586; <https://doi.org/10.1038/s41401-020-00528-w>

## INTRODUCTION

Ca<sup>2+</sup> signals participate in various aspects of life processes [1, 2], including development [3, 4] and cardiac function [5]. Dysregulated Ca<sup>2+</sup> signaling correlates with heart diseases [6, 7]. Thus, the elucidation of Ca<sup>2+</sup> regulatory mechanisms will provide new knowledge in the understanding of heart development, functional maintenance, and disease control.

The cardiac differentiation system of human embryonic stem cells (hESCs) mimics the early developmental process of human hearts [8]. Differentiated cardiomyocytes are structurally and functionally similar to human fetal cardiomyocytes [9, 10]. These properties confer the model of cardiac differentiation of hESCs and derived cardiac lineage cells as a unique model/source for the study of human heart development, heart disease, drug development, and cell therapy [11–15]. However, the contributions of Ca<sup>2+</sup> signals and Ca<sup>2+</sup> handling proteins in the cardiac differentiation of hESCs and derived cardiac lineage cells have not yet been fully clarified.

The endoplasmic reticulum (ER) is a major intracellular Ca<sup>2+</sup> storage site in eukaryotic cells. It plays an important role in

balancing intracellular Ca<sup>2+</sup> homeostasis through Ca<sup>2+</sup> channels and pumps located in the ER membrane [16–20]. Inositol 1,4,5-trisphosphate receptors (IP<sub>3</sub>Rs), which include three subtypes (IP<sub>3</sub>R1, IP<sub>3</sub>R2, and IP<sub>3</sub>R3), and ryanodine receptors, are the two types of Ca<sup>2+</sup> release channels located on the ER membrane. However, IP<sub>3</sub>Rs are the predominant Ca<sup>2+</sup> release channels expressed in ESCs and early differentiating cells from ESCs, since ryanodine receptors are hardly detected at these stages [17, 20–22]. These properties of IP<sub>3</sub>Rs suggest that they might participate in early cell fate decisions. Accordingly, we found that IP<sub>3</sub>R3 deficiency inhibits the cardiac differentiation of mouse (m)ESCs by increasing apoptosis in mesoderm cells [23]. However, in vivo studies have revealed that mice with a single deletion of either *Itpr1*, *Itpr2*, or *Itpr3* display normal cardiogenesis [24]. On the other hand, mice with double deletions of *Itpr1* and *Itpr2* die in utero with defects in the ventricles and atrioventricular canal at embryonic day 11.5 [24, 25]. In addition, triple knockout of all three types of *Itpr* genes enhances cardiomyocyte differentiation but suppresses hematopoietic differentiation of mESCs [26]. These findings suggest that

<sup>1</sup>CAS Key Laboratory of Tissue Microenvironment and Tumor, Laboratory of Molecular Cardiology, Shanghai Institute of Nutrition and Health, University of Chinese Academy of Sciences (CAS) CAS, Shanghai 200031, China; <sup>2</sup>Translational Medical Center for Stem Cell Therapy & Institute for Regenerative Medicine, Shanghai East Hospital, Tongji University School of Medicine, Shanghai 200123, China; <sup>3</sup>School of Chemical Biology and Biotechnology, State Key Laboratory of Chemical Oncogenomics, Peking University Shenzhen Graduate School, Shenzhen 518055, China; <sup>4</sup>Key Laboratory of Medical Electrophysiology of Ministry of Education, Medical Electrophysiology Key Lab of Sichuan province, Institute of Cardiovascular Research, Southwest Medical University, Luzhou 646000, China and <sup>5</sup>Institute for Stem Cell and Regenerative, CAS, Beijing 100101, China  
Correspondence: Huang-tian Yang (htyang@sibs.ac.cn)

Received: 14 May 2020 Accepted: 3 September 2020

Published online: 9 October 2020

the role of *ip<sub>3</sub>rs* in mouse cardiac development is complicated. However, most of our knowledge on the function of IP<sub>3</sub>Rs in cardiac development and cardiomyocytes comes from animal models. The precise function of Ca<sup>2+</sup> signaling and IP<sub>3</sub>Rs in early cardiac development and fetal cardiomyocytes in humans remains largely unknown.

The function of IP<sub>3</sub>Rs in adult cardiomyocytes is also ambiguous. IP<sub>3</sub>R2 has been proposed to be the predominant isoform among the three subtypes of IP<sub>3</sub>Rs in working cardiomyocytes [27, 28]. It has also been shown that IP<sub>3</sub>R2 regulates the firing rate in rabbit ventricular cardiomyocytes [29] and mouse pacemaker cells [30]. However, deletion of IP<sub>3</sub>R2 in mice did not cause obvious changes in baseline cardiac function [24, 31]. The positive inotropic effect of IP<sub>3</sub>R2 in mouse cardiomyocytes by activation of G<sub>q</sub> protein [32, 33] raises the possibility that IP<sub>3</sub>R2 is involved in stress-induced heart disease. This is supported by the upregulation of IP<sub>3</sub>R2 in the hypertrophic and failing heart [33–35]. However, deletion of IP<sub>3</sub>R2 in mice does not alter the progression of dilated cardiomyopathy or pressure overload-induced hypertrophy [31].

IP<sub>3</sub>R2 is expressed in human cardiomyocytes as detected by RNA-seq [36] and Western blot [33], but the roles of IP<sub>3</sub>Rs in human cardiac development and heart function are unclear. We recently found that IP<sub>3</sub>R2 knockout (IP<sub>3</sub>R2KO) significantly inhibits the increase in the intracellular concentration of Ca<sup>2+</sup> stimulated by ATP or UTP in both hESCs and hESC-derived cardiovascular progenitor cells (hCVPCs) [37], suggesting that IP<sub>3</sub>R2 might contribute to the cardiac differentiation of hESCs and the function of hESC-derived cardiomyocytes. In addition, endothelin-1 (ET-1) is highly expressed in ISL1<sup>+</sup> cardiac progenitors in human embryos, and the expansion of ISL1<sup>+</sup> cardiac progenitors derived from hESCs is dependent on ET-1 [38]. Given the direct activation of IP<sub>3</sub>Rs by ET-1 through the G<sub>q</sub> protein [39, 40], it is intriguing to determine the role of IP<sub>3</sub>R2 in the cardiac differentiation of hESCs and in hESC-derived cardiomyocytes.

In the present study, using the *in vitro* cardiomyocyte differentiation model of hESCs combined with IP<sub>3</sub>R2KO hESCs, we examined (i) the role of IP<sub>3</sub>R2 in the generation of CVPCs and cardiomyocytes from hESCs and (ii) the role of IP<sub>3</sub>R2 in the function of ventricular-like cardiomyocytes derived from hESCs. These results increase our knowledge of the contribution of Ca<sup>2+</sup> handling proteins to early cardiac development in humans and to the functional maintenance of early-developing cardiomyocytes.

## MATERIALS AND METHODS

### hESC culture and *in vitro* differentiation

hESC culture was carried out as previously described [37, 41, 42]. Briefly, the hESC H7 cell line (WiCell Research Institute, Madison, WI, USA) was maintained in mTeSR1 medium (Stem Cell Technologies, Vancouver, Canada) on Matrigel (Corning, New York, NY, USA)-coated dishes.

For cardiomyocyte differentiation, hESCs were induced following a modified monolayer differentiation protocol as reported previously [43, 44]. Briefly, hESCs were seeded onto Matrigel-coated 12-well plates at a density of  $2.5 \times 10^4$  cells/cm<sup>2</sup> in mTeSR1 with 10 μmol/L Y-27632 (a ROCK inhibitor, Stem Cell Technologies), and then the medium was changed to one without Y-27632. After the hESCs reached 100% confluence, cardiac differentiation medium (CDM3) containing RPMI-1640 (Gibco, Carlsbad, CA, USA), 213 μg/mL L-ascorbic acid 2-phosphate (Sigma-Aldrich, Carlsbad, USA), and 2 mg/mL bovine serum albumin (Sigma-Aldrich) was used to induce cardiomyocyte differentiation. For the first 2 days of cardiac differentiation, CHIR99021 (a glycogen synthase kinase-3β inhibitor, Stem Cell Technologies) at 6 μmol/L was added to CDM3. Then, the medium was changed to CDM3 supplemented with the Wnt signaling inhibitor IWR-1 (Sigma-Aldrich) at 5 μmol/L

on day 3 and day 4, followed by CDM3 alone until differentiation day 90 (Fig. S1).

For CVPC induction, hESCs were seeded onto Matrigel-coated 6-well plates at a density of  $3.5 \times 10^4$  cells/cm<sup>2</sup> in CVPC induction medium (CIM) for 3 days as reported previously [37, 41, 45]. The CIM contained DMEM/F12, 1×B27 supplement without vitamin A, 1% L-glutamine, 1% penicillin/streptomycin (Life Technologies, Carlsbad, CA, USA), and supplemented with 400 μmol/L L-thioglycerol (Sigma-Aldrich), 50 μg/mL ascorbic acid (Sigma-Aldrich), 25 ng/mL bone morphogenetic protein 4 (R&D Systems, Minneapolis, MN, USA), and 3 μmol/L CHIR99021 (Stem Cell Technologies).

### Flow cytometry analysis

For the cell cycle analysis, cells were stained with 50 μg/mL propidium iodide (Sigma-Aldrich) before analysis. The cells were then analyzed by flow cytometry (Gallios, Beckman Coulter, Brea, CA, USA). The data were analyzed by ModFit software.

For the characterization of CTNT-positive cells, the cells were digested with 0.05% trypsin (Gibco). Then, the cells were fixed and permeabilized by a Foxp3 Staining Buffer kit (Invitrogen). Unconjugated CTNT antibody (1:200, Abcam, Cambridge, UK) was used, followed by staining with PE-Cy7-conjugated secondary antibody (1:400; eBioscience, San Diego, USA). The cells were then analyzed by flow cytometry (Gallios, Beckman Coulter) and quantified by FlowJo software.

### Immunocytochemical staining

Immunocytochemical staining was performed as previously described [42]. Briefly, cells were fixed with 4% PFA, permeabilized with 0.4% Triton X-100 (Sigma-Aldrich), and blocked in 10% goat serum (Vector Laboratories, Burlingame, CA, USA). The primary antibodies used were as follows: OCT4 antibody (1:200, Abcam); SSEA4 antibody (1:200, Millipore, CA, USA); SOX2 antibody (1:200, Abcam); Nkx2.5 antibody (1:200, Santa Cruz Biotechnology, Dallas, TX, USA); ISL1 antibody (1:100; Developmental Studies Hybridoma Bank, Iowa City, IA, USA); CTNT antibody (1:200, Abcam); MLC2V antibody (1:100, Abcam) and α-ACTININ antibody (1:400, Sigma-Aldrich). Alexa 488- or 569-conjugated secondary antibody (Invitrogen) was used for detection. Nuclei were stained with DAPI (Sigma-Aldrich). Images were captured by a Zeiss LSM 710 confocal microscope.

### Quantitative reverse transcription polymerase chain reaction (qRT-PCR)

Total RNA was extracted with a RNeasy Mini kit (QIAGEN, Hilden, Germany) following the manufacturer's instructions and then reverse-transcribed by using ReverTra Ace reverse transcriptase (Toyobo, Osaka, Japan). qRT-PCR was performed using the ViiA 7 Real-Time PCR System (Life Technologies) with SYBR Green qPCR Master Mix (Roche, Mannheim, Germany). The results are presented as fold changes normalized to *GAPDH*. The qRT-PCR primers are listed in Table S1.

### Western blot analysis

The cells were harvested and lysed in lysis buffer containing 8 mol/L urea, 2 mol/L thiourea, 3% sodium lauryl sulfate, 75 mmol/L 1,4-dithiothreitol, 50 mmol/L TRIS, and 0.03% bromophenol blue (pH adjusted to 6.8) (Sigma-Aldrich). The antibodies against IP<sub>3</sub>R1 and IP<sub>3</sub>R2 were generated as previously reported [46]. The membranes were incubated with primary antibodies against IP<sub>3</sub>R1 (1:1000), IP<sub>3</sub>R2 (1:1000), IP<sub>3</sub>R3 (1:1000, BD Biosciences, San Jose, CA, USA), GAPDH (1:20000, Proteintech, Rosemont, IL, USA), and β-actin (1:8000; Sigma-Aldrich) in 3% BSA. IRDye 680LT donkey anti-rabbit IgG or IRDye 800LT donkey anti-mouse IgG (1:8000; Li-COR Biosciences, Lincoln, NE, USA) was used for detection. Images were captured using an Odyssey Infrared Imager (Li-COR Biosciences).

### Karyotype analysis

Karyotype analysis was conducted as previously reported [47]. Briefly, hESCs were treated with colchicine (100 µg/mL) for 3 h at 37 °C and then harvested as single cells. The cells were hypotonic in 75 mmol/L KCl at 37 °C for 30 min and then fixed by freshly prepared fixative (glacial acetic acid:methanol = 1:3). After dropping the solution onto clean slides, the samples were stained with Giemsa staining solution. Twenty metaphase cells were counted, of which five cells were analyzed and karyotyped in each cell line.

### Recording of Ca<sup>2+</sup> transients

Cardiomyocytes derived from hESCs at differentiation day 90 were digested using 0.05% trypsin and plated in glass bottom cell culture dishes (Wuxi NEST Biotechnology, Wuxi, China). After 24 to 48 h of plating, the cells were loaded with 2 µmol/L Fluo4-AM (Life Technologies) dissolved in Tyrode's buffer for 15 min at room temperature (RT). Tyrode's buffer contained (in mmol/L) NaCl, 135; KCl, 5.4; CaCl<sub>2</sub>, 1.8; MgCl<sub>2</sub>, 1.0; glucose, 10; and HEPES, 10 (pH adjusted to 7.4). Then, the Ca<sup>2+</sup> indicator was washed off 3 times, and the cells were incubated at RT for 15 min before use. The Ca<sup>2+</sup> transients were captured in the line scan model using a Zeiss LSM 710 confocal microscope. A total of 5000 lines with an interval time of 10 ms were scanned. During the recording, the cells were maintained at 35 °C in a heated chamber. Phenylephrine (PE) (an α<sub>1</sub>-adrenergic receptor agonist) was used at 10 µmol/L. The Ca<sup>2+</sup> transients were analyzed with IDL software (ITT Corporation, White Plains, NY, USA).

### Recording of action potentials (APs)

APs were recorded as previously described [48]. Briefly, cardiomyocytes derived from hESCs at differentiation day 90 were digested and replated onto coverslips. The cells were then recorded for APs within 24–48 h after plating. The temperature was maintained at 33 °C by perfusion with warm Tyrode's buffer by a peristaltic pump (Cole-Parmer, IL, USA). The internal solution contained (in mmol/L): K<sup>+</sup>-aspartate, 110; KCl, 20; MgCl<sub>2</sub>, 1; NaGTP, 0.1; MgATP, 5; Na<sub>2</sub>-phosphocreatine, 5; EGTA, 1; and HEPES, 10; pH adjusted to 7.3 with KOH. APs were recorded using the EPC-10 amplifier (Heka Electronics, Bellmore, NY, USA) in current-clamp mode. PE was used at 10 µmol/L. The characterization of the cardiomyocyte subtypes was based on previously reported criteria [44]. Briefly, for ventricular-like cardiomyocytes, AP amplitude > 90 mV, AP duration at 90% repolarization/AP duration at 50% repolarization (APD<sub>90</sub>/APD<sub>50</sub>) < 1.4, a rapid AP upstroke, a long plateau phase, and a negative maximum diastolic potential (MDP) (< -48 mV); for atrial-like cardiomyocytes, an absence of a prominent plateau phase, a negative diastolic membrane potential (< -48 mV) and APD<sub>90</sub>/APD<sub>50</sub> > 1.7; and for Nodal-like cardiomyocytes, a more positive MDP, a slower AP upstroke, a prominent phase 4 depolarization and APD<sub>90</sub>/APD<sub>50</sub> between 1.4 and 1.7.

### Statistical analysis

The data are presented as the mean ± SEM. One-way analysis of variance (ANOVA) followed by Bonferroni's multiple analysis was used for the qRT-PCR assay of *ITPRs*, cell cycle distribution and flow cytometry analysis of CTNT. Two-way ANOVA with Bonferroni's multiple comparison test was used to analyze the qRT-PCR data for the expression of different genes during cardiomyocyte differentiation and the quantitative properties of APs and Ca<sup>2+</sup> transients of the three cell lines. A paired *t* test was used to analyze the quantitative properties of APs and Ca<sup>2+</sup> transients with or without PE. All of the statistical analyses were conducted using GraphPad Prism8. *P* < 0.05 was considered statistically significant.

## RESULTS

### Differentiation of hESCs to dominant ventricular-like cardiomyocytes

To determine the role of IP<sub>3</sub>R2 in the fate of human ventricular cardiomyocytes and the function of hESC-derived cardiomyocytes, we differentiated hESCs into cardiomyocytes following a protocol reported previously [43, 44] with a small modification (Fig. S1a). Spontaneously beating cardiomyocytes appeared on differentiation day 7, and robust beating cardiomyocytes were observed on differentiation day 8 (Movie S1). Flow cytometry analysis confirmed that over 90% of cells were positive for the cardiac-specific marker CTNT at differentiation day 90 (Fig. S1b). The differentiated cardiomyocytes showed a well-arranged sarcomere structure (Fig. S1c). To determine the subtypes of differentiated cardiomyocytes, we recorded the APs of the cells at differentiation day 90. The examined cardiomyocytes derived from wild-type (wt) hESCs showed typical ventricular-like APs (Fig. S1d) with an APD<sub>90</sub>/APD<sub>50</sub> ratio of 1.17 ± 0.01 (Fig. S1e) based on previously reported criteria [44]. These data demonstrate that cardiomyocytes differentiated from hESCs around day 90 are mainly ventricular-like cardiomyocytes.

IP<sub>3</sub>R2 is highly expressed in undifferentiated hESCs and downregulated in differentiated cardiomyocytes

Next, we examined the expression profile of IP<sub>3</sub>R2 during cardiomyocyte differentiation. qRT-PCR analysis showed that the *ITPR2* gene was highly expressed in undifferentiated hESCs and was quickly downregulated during the first 2 days of differentiation. Then, it was upregulated at differentiation days 3 and 4 and gradually downregulated in the following days, reaching a relatively stable level from differentiation day 6 to day 90 (Fig. 1a). A similar pattern of IP<sub>3</sub>R2 protein was observed during cardiac differentiation of hESCs by Western blot analysis (Fig. 1b).

Deficiency in IP<sub>3</sub>R2 does not significantly affect the self-renewal of hESCs

To determine the role of IP<sub>3</sub>R2 in cardiac differentiation, we used two IP<sub>3</sub>R2KO hESC lines (IP<sub>3</sub>R2KO-6 and IP<sub>3</sub>R2KO-12) generated by using transcription activator-like effector nuclease (TALEN) technology as previously reported [37]. All of the wt, IP<sub>3</sub>R2KO-6 and IP<sub>3</sub>R2KO-12 hESCs showed the normal karyotype (Fig. S2). The deficiency in IP<sub>3</sub>R2 was confirmed in IP<sub>3</sub>R2KO-6 and IP<sub>3</sub>R2KO-12 lines by Western blot, while the protein levels of other subtypes of IP<sub>3</sub>Rs, i.e., IP<sub>3</sub>R1 and IP<sub>3</sub>R3 (encoded by the *ITPR1* and *ITPR3* gene, respectively), were not affected (Fig. 2a), which was consistent with the qRT-PCR analysis (Fig. 2b).

We previously found that IP<sub>3</sub>R2 is a dominantly functional Ca<sup>2+</sup> channel for mediating Ca<sup>2+</sup> release from the ER in both mESCs [49] and hESCs [22, 37]. To test whether IP<sub>3</sub>R2 deficiency affects the self-renewal of hESCs, we conducted alkaline phosphatase (ALP) staining, immunocytochemical staining and qRT-PCR. All wt, IP<sub>3</sub>R2KO-6 and IP<sub>3</sub>R2KO-12 hESCs were positive for ALP, OCT4, SSEA4 and SOX2 (Fig. 2c). The mRNA levels of *POU5F1* (encodes OCT4), *NANOG* and *SOX2* were also comparable between these three hESC lines (Fig. 2d). Furthermore, flow cytometry analysis did not detect a difference in the cell cycle distribution among the wt and two IP<sub>3</sub>R2KO cell lines (Fig. 2e, f). Therefore, IP<sub>3</sub>R2 seems to be dispensable for the maintenance of hESC self-renewal.

IP<sub>3</sub>R2 is dispensable for the differentiation of hESCs into CVPCs and cardiomyocytes

The upregulated expression of IP<sub>3</sub>R2 from differentiation day 3 to day 4 suggests a possible contribution of IP<sub>3</sub>R2 in mediating cardiac progenitor formation, as this is a critical stage for the transition of cardiac mesoderm to cardiac progenitors [44]. To determine the effect of IP<sub>3</sub>R2 on the generation of CVPCs from hESCs, we induced wt and IP<sub>3</sub>R2KO cells to differentiate into

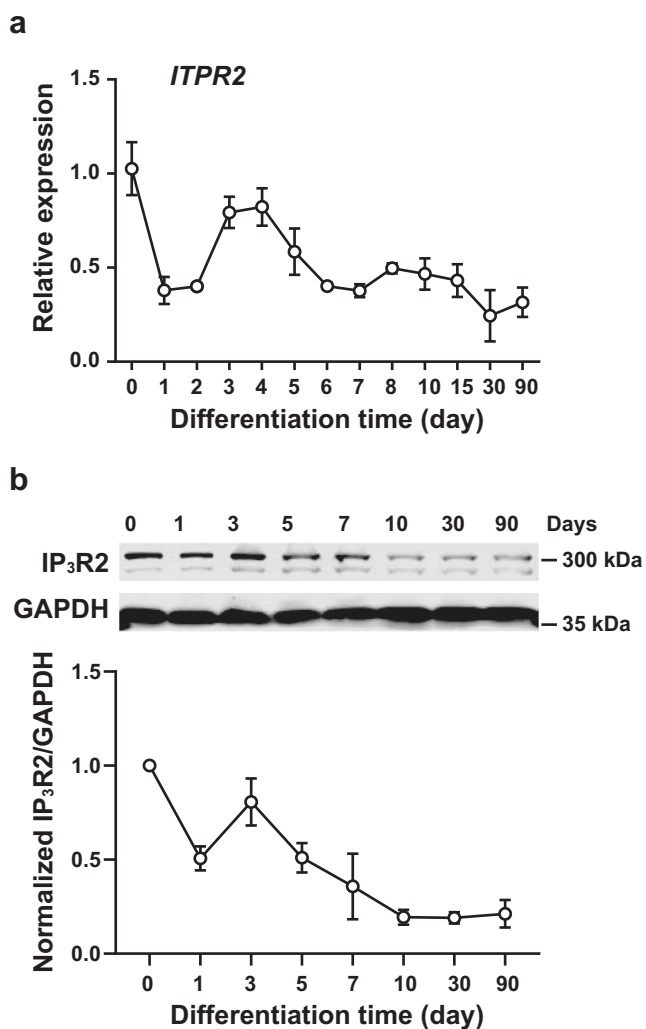


**Fig. 1** The expression pattern of IP<sub>3</sub>R2 during cardiomyocyte differentiation of hESCs. **a** qRT-PCR analysis of the expression of the *ITPR2* gene. *n* = 3. **b** Western blot analysis of IP<sub>3</sub>R2 protein levels. GAPDH was used as the loading control. *n* = 3.

CVPCs by using a protocol established by our group [41, 45]. Immunocytochemical staining showed that all of the differentiating cells from the wt and IP<sub>3</sub>R2KO cells uniformly expressed the primitive CVPC markers NKX2-5 and ISL1 in the nuclei (Fig. 3a). Next, to determine whether IP<sub>3</sub>R2 affects cardiomyocyte generation, wt and IP<sub>3</sub>R2KO hESCs were further induced to differentiate into cardiomyocytes. We found that the percentages of CTNT-positive cells were comparable between the wt and the two IP<sub>3</sub>R2KO cell lines at differentiation day 90 (Fig. 3b). The clear and organized sarcomeric structure of induced cardiomyocytes was similar among the wt and IP<sub>3</sub>R2KO cells (Fig. 3c). In addition, the cells were double positive for MLC2V and  $\alpha$ -ACTININ (Fig. 3d). Notably, the fiber-like structures observed in the green and red channels were well colocalized (Fig. 3d), indicating that these cells were ventricular-like myocytes. These data are consistent with the observations of the typical ventricular-like myocyte APs shown in Fig. S1d and S1e. qRT-PCR analysis further confirmed that the genes were sequentially expressed following a tandem transition from pluripotency (*POU5F1*), mesoderm (*TBX7*), cardiac mesoderm (*MESP1*), cardiac progenitor (*ISL1* and *NKX2-5*) to cardiomyocytes (*TNNT2*) in the wt and two IP<sub>3</sub>R2KO cell lines (Fig. 3e). These data suggest that IP<sub>3</sub>R2 deficiency does not

significantly affect the induction of CVPCs and cardiomyocytes from hESCs.

IP<sub>3</sub>R2KO mildly alters APs by stimulating  $\alpha_1$ -adrenergic receptors in hESC-derived cardiomyocytes

As the functional contribution of IP<sub>3</sub>R2 remains controversial in adult working cardiomyocytes [24, 33] and is unknown in early differentiated human cardiomyocytes, we examined whether IP<sub>3</sub>R2 affects APs, a crucial feature of beating cardiomyocytes [50]. The spontaneously beating cardiomyocytes at differentiation day 90 showed typical ventricular-like APs (Fig. 4a), with small variations in the MDP and amplitude but large variations in the beats per minute (Bpm), maximum rate of rise ( $V_{max}$ ) and depolarization ( $D_{max}$ ), APD50 and APD90 in the examined cardiomyocytes (Fig. 4b–h). The features of APs in cardiomyocytes derived from IP<sub>3</sub>R2KO hESCs were similar to those in the wt hESCs (Fig. 4a). To confirm this, we quantitatively analyzed the parameters of APs in these cells (Fig. 4b–h). The Bpm, amplitude, MDP,  $V_{max}$ ,  $D_{max}$ , APD50, and APD90 in cardiomyocytes derived from IP<sub>3</sub>R2KO hESCs were comparable to those in the wt cardiomyocytes. Next, we examined whether IP<sub>3</sub>R2 deficiency affects APs under the stimulation of PE, an  $\alpha_1$ -adrenergic receptor agonist that activates IP<sub>3</sub>Rs through the  $G_q$  protein [51, 52]. Spontaneous APs from the same cardiomyocyte with and without PE treatment were recorded. PE stimulation significantly accelerated the beating frequency (Fig. 4a, b), accompanied by increased MDP (Fig. 4d) and decreased amplitude (Fig. 4c),  $V_{max}$  (Fig. 4e), APD50 (Fig. 4g), and APD90 (Fig. 4h), while  $D_{max}$  was unchanged (Fig. 4f) compared with the corresponding values in wt hESC-derived cardiomyocytes without PE treatment. In the IP<sub>3</sub>R2KO hESC-derived cardiomyocytes, the Bpm, MDP,  $V_{max}$ , APD50, and APD90 were comparable with those in the wt cardiomyocytes (Fig. 4b, d, e, g, h). However, it is notable that the amplitude in IP<sub>3</sub>R2KO-12 cardiomyocytes was decreased by 4.5% compared with that of wt cardiomyocytes, and a similar tendency was observed in IP<sub>3</sub>R2KO-6 cardiomyocytes without statistical significance (Fig. 4b). In addition, the  $D_{max}$  in IP<sub>3</sub>R2KO-6 cardiomyocytes was approximately 17% slower than that in wt cardiomyocytes, and the same tendency was observed in IP<sub>3</sub>R2KO-12 cardiomyocytes (Fig. 4f). Overall, IP<sub>3</sub>R2KO does not alter spontaneous APs under baseline conditions, but it appears to contribute to the amplitude and  $D_{max}$  of APs in hESC-derived cardiomyocytes under the stimulation of  $\alpha_1$ -adrenergic receptors.

IP<sub>3</sub>R2KO does not significantly affect Ca<sup>2+</sup> transients in hESC-derived cardiomyocytes

We next examined the contributions of IP<sub>3</sub>R2 to Ca<sup>2+</sup> transients in hESC-derived cardiomyocytes. The rhythmic Ca<sup>2+</sup> transients were observed in spontaneously beating cardiomyocytes (Fig. 5a). The parameters of Ca<sup>2+</sup> transients among wt cardiomyocytes, such as the Bpm (Fig. 5b), amplitude (Fig. 5c), time to peak (Fig. 5d), time of decay to 90% (Fig. 5e) and 63% peak (T-90% decay and T-63% decay) (Fig. 5f), varied over a wide range as observed in the APs. The various parameters of Ca<sup>2+</sup> transients in the cardiomyocytes derived from IP<sub>3</sub>R2KO hESCs were similar to those in wt cells (Fig. 5a–f). With PE treatment, the Bpm was significantly increased in wt cardiomyocytes, accompanied by decreases in time to peak, T-90% decay, and T-63% decay, while the amplitude was unchanged (Fig. 5a–f). In the cardiomyocytes derived from the two IP<sub>3</sub>R2KO hESC lines, the Bpm, amplitude, time to peak, T-90% decay and T-63% decay were comparable with those in the wt cell lines (Fig. 5b–f). Collectively, these data indicate that the stimulation of  $\alpha_1$ -adrenergic receptors significantly increases the speed rising to the peak and recovery of Ca<sup>2+</sup> transients in hESC-derived cardiomyocytes, although a large variation exists among cardiomyocytes. Moreover, IP<sub>3</sub>R2 deficiency does not significantly affect Ca<sup>2+</sup> transients in hESC-derived cardiomyocytes with or without  $\alpha_1$ -adrenergic stimulation.

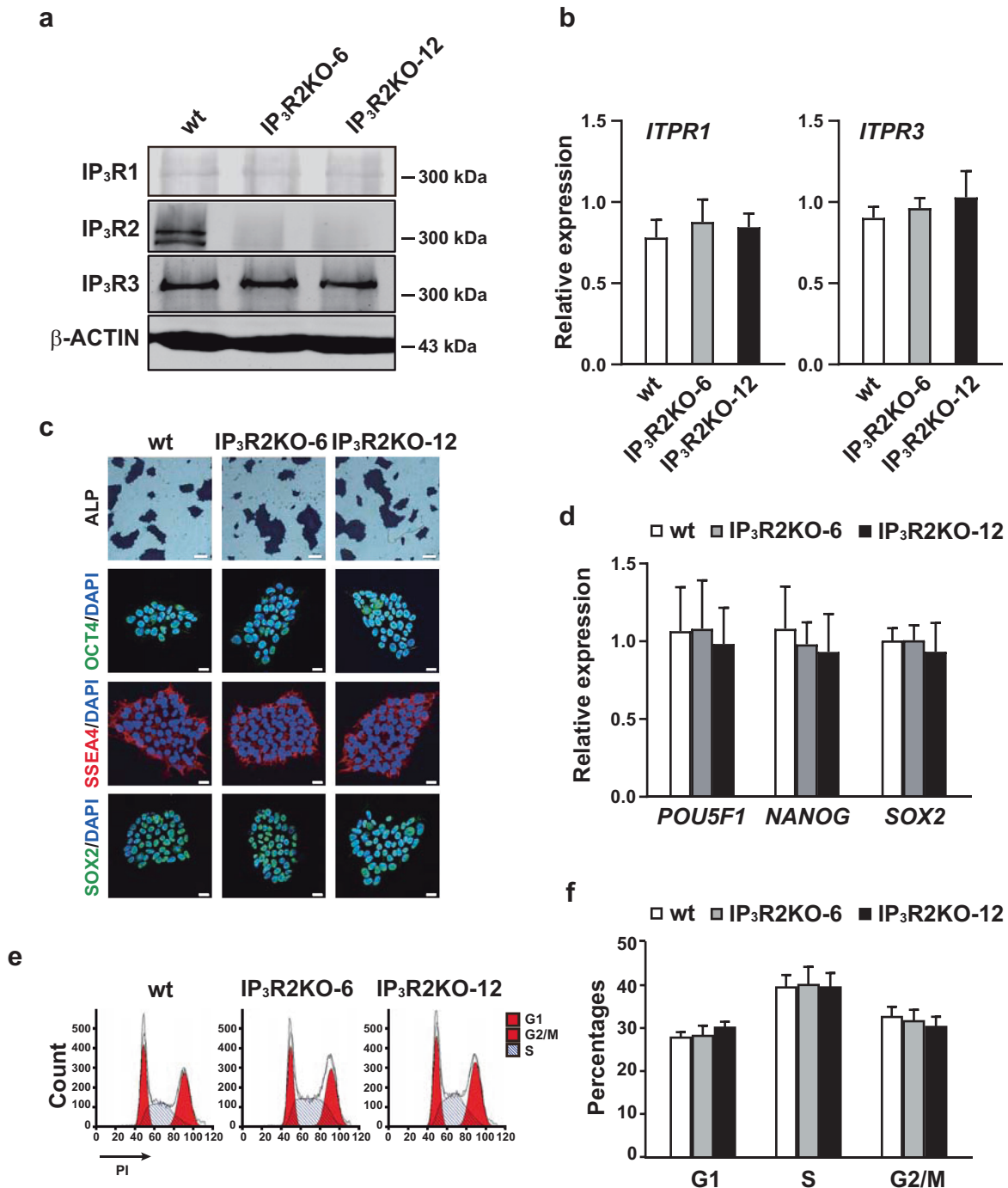


**Fig. 2** The comparison of self-renewal properties of undifferentiated wt, IP<sub>3</sub>R2KO-6, and IP<sub>3</sub>R2KO-12 hESCs. **a** Western blot analysis of IP<sub>3</sub>R1, IP<sub>3</sub>R2 and IP<sub>3</sub>R3 proteins. β-actin was used as the loading control. **b** qRT-PCR analysis of *ITPR1* and *ITPR3* gene expression. *n* = 3. **c** The alkaline phosphatase staining and immunocytochemical staining of OCT4, SSEA4 and SOX2. Scale bar = 100 μm (ALP). Scale bar = 10 μm (immunocytochemical staining). **d** qRT-PCR analysis of *POU5F1*, *NANOG* and *SOX2* gene expression. **e** The representative flow cytometry plots of cell cycle analysis. **f** The cell cycle analysis data. *n* = 3.

## DISCUSSION

In this study, using the in vitro hESC cardiac differentiation model, combined with IP<sub>3</sub>R2 knockout, Ca<sup>2+</sup> imaging, and AP recording, we determined (i) the expression pattern of IP<sub>3</sub>R2 during cardiomyocyte differentiation of hESCs; (ii) IP<sub>3</sub>R2 deficiency does not affect the self-renewal of hESCs; (iii) IP<sub>3</sub>R2 deficiency does not significantly affect CVPC and cardiomyocyte differentiation from hESCs; (iv) hESC-derived cardiomyocytes have ventricular-like APs but with large variations in the parameters of APs and Ca<sup>2+</sup>

transients under both baseline conditions and the stimulation of α<sub>1</sub>-adrenergic receptors; (v) IP<sub>3</sub>R2 deficiency decreases the amplitude and the *D*<sub>max</sub> of APs in hESC-derived cardiomyocytes under the stimulation of α<sub>1</sub>-adrenergic receptors but not under baseline conditions; and (vi) no obvious changes are observed in the Ca<sup>2+</sup> transients in IP<sub>3</sub>R2KO cardiomyocytes with or without the stimulation of α<sub>1</sub>-adrenergic receptors. Our results suggest the minimal contribution of IP<sub>3</sub>R2 in cardiac differentiation and derived ventricular cardiomyocytes from hESCs.

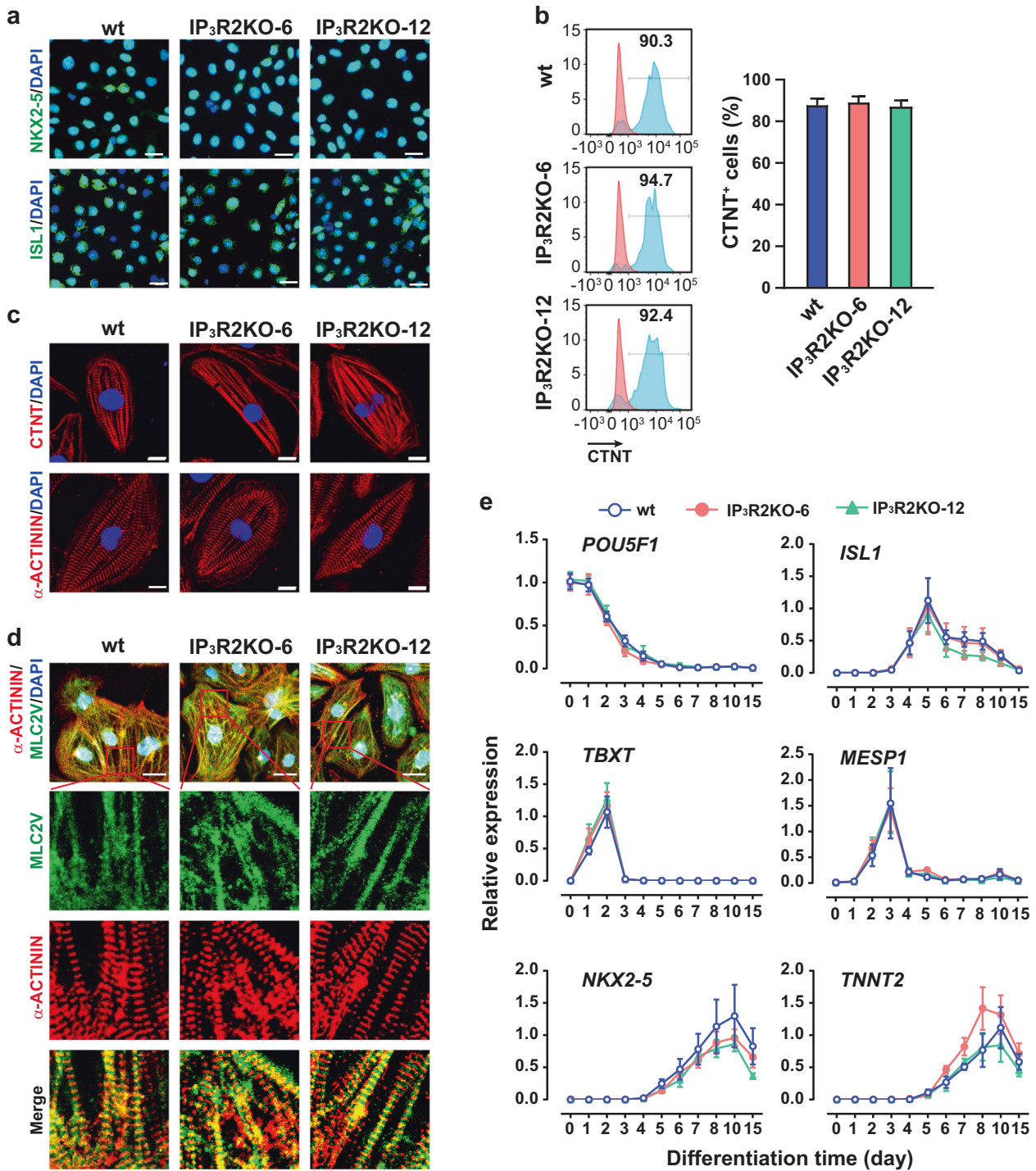


**Fig. 3** Effects of IP<sub>3</sub>R2 deficiency on the differentiation of hESCs into CVPCs and cardiomyocytes. **a** Immunocytochemical staining analysis of CVPC marker NKX2-5 and ISL1 in induced CVPCs. Scale bar = 40 μm. **b** Flow cytometry analysis of cardiomyocytes induced from wt, IP<sub>3</sub>R2KO-6 and IP<sub>3</sub>R2KO-12 hESCs with cardiomyocyte marker CTNT. *n* = 3. **c** Immunocytochemical staining analysis of cardiomyocyte marker CTNT and α-ACTININ in cardiomyocytes at differentiation day 90. Scale bar = 10 μm. **d** Co-immunocytochemical staining analysis of cardiomyocyte marker α-ACTININ and ventricular myocyte marker MLC2V at cardiac differentiation day 90. Scale bar = 20 μm. **e** The mRNA expression of genes during cardiac differentiation from hESCs. *POU5F1*, pluripotency marker; *TBXT*, early mesoderm marker; *MESP1*, cardiac mesoderm marker; *ISL1* and *NKX2-5*, cardiac progenitor markers; *TNNT2*, cardiomyocyte marker. *n* = 3.

One of the findings here is the determination of the expression patterns of IP<sub>3</sub>R2 during the process of cardiomyocyte generation from hESCs. This observation is consistent with previous findings of the presence of IP<sub>3</sub>R2 in undifferentiated hESCs, hESC-derived CVPCs [22, 37] and human adult cardiomyocytes [33]. Our findings support previous observations and precisely describe the specific

expression patterns of IP<sub>3</sub>R2 during the differentiation process of hESCs into cardiomyocytes, especially for ventricular-like myocytes, by revealing the following characteristics. First, the expression of IP<sub>3</sub>R2 is downregulated during the formation and maturation of cardiomyocytes from hESCs. This pattern is similar to those previously observed in the generation of CVPCs [37] and

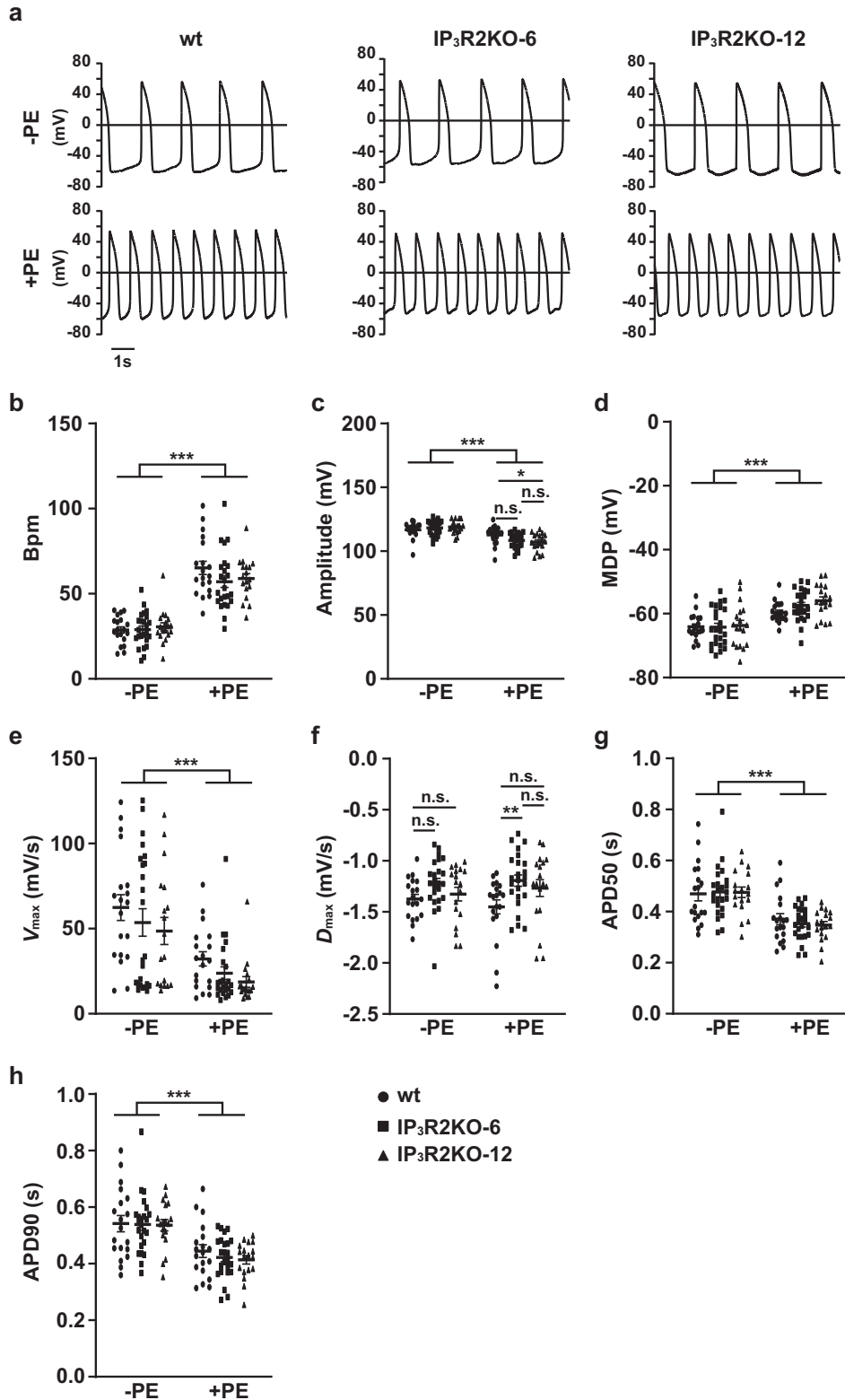


**Fig. 4** Effects of IP<sub>3</sub>R2 deficiency on the APs of wt and IP<sub>3</sub>R2KO hESC-derived cardiomyocytes at differentiation day 90 with or without phenylephrine (PE) treatment. **a** Representative AP recordings. **b–h** Parameters of APs. Bpm, beats per minute (**b**); Amplitude (**c**); MDP, maximum diastolic potential (**d**);  $V_{max}$ , the maximum rate of rise of the AP (**e**);  $D_{max}$ , the maximum rate of depolarization (**f**); APD50, AP duration at 50% repolarization (**g**); APD90, AP duration at 90% repolarization (**h**). PE, phenylephrine at 10  $\mu$ mol/L concentration.  $n = 19$  for wt cardiomyocytes;  $n = 24$  for IP<sub>3</sub>R2KO-6 cardiomyocytes;  $n = 18$  for IP<sub>3</sub>R2KO-12 cardiomyocytes. \* $P < 0.05$ , \*\* $P < 0.01$ , \*\*\* $P < 0.001$ . n.s., no significant difference.

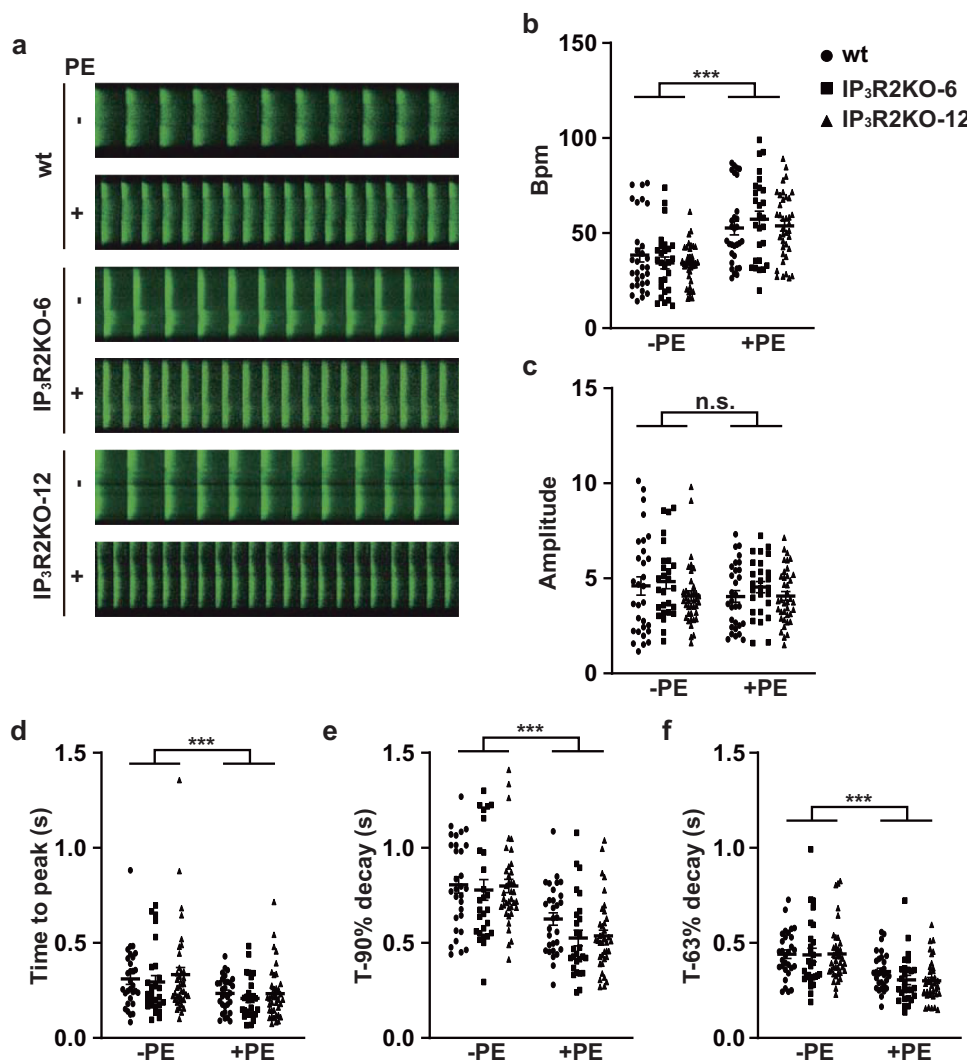


**Fig. 5** Effects of IP<sub>3</sub>R2 deficiency on Ca<sup>2+</sup> transients of wt and IP<sub>3</sub>R2KO hESC-derived cardiomyocytes at differentiation day 90 with or without phenylephrine (PE) treatment. **a** Representative images of spontaneous intracellular Ca<sup>2+</sup>. **b–e** Parameters of spontaneous Ca<sup>2+</sup> transients. The Bpm (**b**), amplitude ( $\Delta F/F_0$ , **c**), time to peak (**d**), time to 90% decay (**e**), and time to 63% decay (**f**) of the maximum amplitude.  $n = 30$  for wt cardiomyocytes;  $n = 27$  for IP<sub>3</sub>R2KO-6 cardiomyocytes;  $n = 38$  for IP<sub>3</sub>R2KO-12 cardiomyocytes. \*\*\* $P < 0.001$  compared with the corresponding control group cells.

cardiomyocytes [53] from hESCs. However, notably, at the early differentiation stage (differentiation day 0 to day 1, representing the transition stage of undifferentiated hESCs to mesoderm cells), the expression of IP<sub>3</sub>R2 was sharply downregulated, followed by upregulation at differentiation days 3 and 4 (representing the transition stage from mesoderm to cardiac mesoderm)(Fig. 1). This correlation between the expression of IP<sub>3</sub>R2 and cell fate transition suggests the possible role of IP<sub>3</sub>R2 in human lineage fate determination. Although it is unknown whether this transient down- and upregulation is involved in the tissue-specific lineage fate determination in humans, our previous study showed that the abundance of IP<sub>3</sub>R3 is transiently downregulated in the early differentiation stage of mESCs and that knockdown of IP<sub>3</sub>R3 in mESCs significantly suppresses the differentiation into mesoderm and cardiomyocytes by specifically increasing the apoptosis of mesodermal cells due to the alternation of Ca<sup>2+</sup> oscillation [23]. Considering the evidence for the existence of IP<sub>3</sub>Rs in both hESCs [22, 37] and mESCs [23, 26, 54] and the functional overlap or negative feedback among these subtypes [1, 23, 25, 26, 55–57], the significance of the transient downregulation of IP<sub>3</sub>R2 to the specific cell fate decision during early differentiation of hESCs

needs to be elucidated in the future. Moreover, in this study, we demonstrate that the IP<sub>3</sub>R2 protein exists in hESC-derived ventricular-like myocytes. We confirmed that the efficiently generated cardiomyocytes from hESCs have ventricular myocyte-like APs (Fig. S1d) and are positive for the ventricular marker MLC2V (Fig. 3d). Therefore, IP<sub>3</sub>R2 exists in both differentiated human ventricular-like myocytes (Fig. 1) and human adult left ventricular myocytes [33].

Interestingly, although IP<sub>3</sub>R2 is highly expressed in undifferentiated hESCs, it has little contribution to the maintenance of hESC self-renewal. However, the percentage of cells responding to MRS2365, a G<sub>q</sub> protein-coupled P2Y<sub>1</sub> receptor agonist, is significantly decreased in IP<sub>3</sub>R2KO hESCs [37], indicating the important role of IP<sub>3</sub>R2 in mediating Ca<sup>2+</sup> release from intracellular stores in hESCs. A possible interpretation for these observations might be that IP<sub>3</sub>R2 deficiency could be compensated by other subtypes of IP<sub>3</sub>Rs or Ca<sup>2+</sup> modulators. Although the robust Ca<sup>2+</sup> waves are mediated by IP<sub>3</sub>R2, the intracellular Ca<sup>2+</sup> concentration is stable with minor fluctuations in undifferentiated hESCs [22]. Thus, the small fluctuations might be enough for the maintenance of hESCs in the steady state. Moreover, in IP<sub>3</sub>R2KO



hESCs, there are still some cells responding to MRS2365, despite a low percentage (<20%) [37], suggesting that IP<sub>3</sub>R3 might compensate for the loss of IP<sub>3</sub>R2. In addition, the intracellular Ca<sup>2+</sup> channels and Ca<sup>2+</sup> modulators located in the plasma membrane might also participate in the Ca<sup>2+</sup> homeostasis maintained after IP<sub>3</sub>R2 deficiency. Therefore, the self-renewal property of IP<sub>3</sub>R2KO hESCs is maintained. Accordingly, the functional redundancy of IP<sub>3</sub>R subtypes is also detected in mice. The *Itpr1*, *Itpr2*, or *Itpr3* single mutants were indistinguishable from the control mice. No contribution of IP<sub>3</sub>R2 to CVPC and cardiomyocyte generation could also be caused by the redundancy of other IP<sub>3</sub>R subtypes and Ca<sup>2+</sup> modulators. Indeed, cardiac progenitor and cardiomyocyte differentiation is enhanced, but the hematopoietic mesoderm is reduced in mESCs with triple knockout of *Itpr1*, *Itpr2*, and *Itpr3* [26]. Although it has been reported that ET-1, which can activate IP<sub>3</sub>Rs through endothelin receptors [39, 40], is crucial in promoting the expansion of ISL1<sup>+</sup> cardiac progenitors from hESCs [38], the underlying mechanisms are not elucidated. Moreover, a recent report [58] argues that the heart defect is caused by double knockout of *Itpr1* and *Itpr2* [24]. Yang and colleagues [58] found that specific deletion of *Itpr1* and *Itpr2* in cardiomyocytes, endothelial/hematopoietic cells or early cardiovascular lineage progenitor cells of mice do not have phenotypes, while the embryonic lethality caused by double knockout of *Itpr1* and *Itpr2* may be due to allantoic-placental defects. Thus, the vascular abnormalities seen in *Itpr1* and *Itpr2* double knockout mice might not be due to the indirect influence but are a secondary effect on allantoic/placental defects. Overall, IP<sub>3</sub>R2 deficiency alone does not affect cardiomyocyte differentiation in mice or humans.

Another interesting finding here is that the positive chronotropic effect of PE is not affected by IP<sub>3</sub>R2 deficiency, and only mild changes in the amplitude and  $D_{max}$  of the APs in IP<sub>3</sub>R2KO hESC-derived cardiomyocytes under PE stimulation are observed compared with those in wt cardiomyocytes (Fig. 4c, f). The positive chronotropic effect of PE in immature cardiomyocytes is mediated by  $\alpha_1$ -adrenergic receptors [59]; however, the underlying mechanism remains unknown. The positive chronotropic effect induced by  $\beta$ -adrenergic receptor activation is related to the regulation of Ca<sup>2+</sup> influx through the L-type Ca<sup>2+</sup> channel [60–63]. This channel is also regulated by the activation of  $\alpha_1$ -adrenergic receptors [64]. Thus, the chronotropic effect of PE in immature cardiomyocytes might also be mediated through L-type Ca<sup>2+</sup> channels, although we could not exclude the participation of other channels, such as sodium channels or potassium channels. In addition, given that IP<sub>3</sub>R2 can be located near the plasma membrane [28, 30, 53, 65], IP<sub>3</sub>R2 might affect the voltage-gated ion channels on the plasma membrane by regulating the surrounding electrical environment, as hypothesized [66, 67], and this possibility needs to be tested.

Despite the possible role of IP<sub>3</sub>R2 in the regulation of ion channels, the contribution of IP<sub>3</sub>R2 to the functional properties of hESC-derived cardiomyocytes is weak. Under basal conditions, the APs and Ca<sup>2+</sup> transients of the cardiomyocytes derived from wt and IP<sub>3</sub>R2KO hESCs are similar. It has been shown that IP<sub>3</sub>Rs contribute to the regulation of Ca<sup>2+</sup> transients and/or contraction in mESC- [49] or hESC-derived cardiomyocytes [53, 65], isolated rabbit ventricular myocytes [28, 29], and adult human ventricular cardiomyocytes [33]. However, these conclusions are mainly based on the usage of agonists and antagonists of IP<sub>3</sub>Rs, lacking confirmation by using direct gene interference. Therefore, the nonspecific effects of these reagents could not be excluded. For example, the commonly used pan-IP<sub>3</sub>R antagonist 2-APB can also inhibit Ca<sup>2+</sup> release-activated Ca<sup>2+</sup> channels [68]. Thus, the results collected from studies without direct gene interference should be carefully interpreted. In the present study, the significant chronotropic response to the activation of  $\alpha_1$ -adrenergic receptors with PE in wt cardiomyocytes is consistent with a previous

report [59, 69], while the amplitude of Ca<sup>2+</sup> transients remained unchanged under the stimulation of  $\alpha_1$ -adrenergic receptors. However, activation of other G<sub>q</sub>-coupled receptors in cardiomyocytes, such as ET-1 receptors and purinergic receptors, correlates with enhanced Ca<sup>2+</sup> transients and increased contractility [33, 70]. Such differences may be due to the diversity of downstream cascades of different receptors. These possibilities need to be tested further. Notably, the PE-induced chronotropic response remained unchanged in IP<sub>3</sub>R2KO cardiomyocytes. This may have several interpretations. (i) IP<sub>3</sub>R2 minimally contributes to the function of hESC-derived cardiomyocytes. This is supported by the findings that heart function is normal in IP<sub>3</sub>R2-deficient mice [24, 31]. (ii) The functional redundancy of other IP<sub>3</sub>R subtypes may compensate for the loss of function of IP<sub>3</sub>R2. (iii) The large variations in the different parameters of APs and Ca<sup>2+</sup> transients indicate the heterogeneous maturation of hESC-derived cardiomyocytes, which may conceal the mild involvement of IP<sub>3</sub>R2 in the function of early cardiomyocytes. Accordingly, the amplitude and recovery of APs under the activation of  $\alpha_1$ -adrenergic receptors were altered in IP<sub>3</sub>R2KO cardiomyocytes. (iv) Lastly, IP<sub>3</sub>R2 might be involved in the regulation of cardiomyocyte function under long-term stimulation. In the current study, APs were recorded immediately after PE addition, reflecting the acute response of cardiomyocytes. In a mouse model, the overexpression of  $\alpha_{1A}$ -adrenergic receptor [71] or IP<sub>3</sub>R2 [35] results in cardiac hypertrophy, suggesting that the chronic activation of IP<sub>3</sub>R2 might act as a pathological stimulus to the heart. In this circumstance, the relationship of the mild changes of the APs with the pathological outcomes under the chronic activation of IP<sub>3</sub>R2 needs to be studied in the future.

In conclusion, we have determined the precise expression pattern of IP<sub>3</sub>R2 during cardiomyocyte differentiation of hESCs and demonstrated that IP<sub>3</sub>R2 is dispensable in the self-renewal and cardiac differentiation of hESCs. IP<sub>3</sub>R2 has minimal contribution to the function of hESC-derived ventricular-like cardiomyocytes. These findings provide new insights into the role of IP<sub>3</sub>Rs in human early cardiac development and in human immature ventricular myocytes. This knowledge would also provide references for the use of hESC-derived cardiomyocytes as disease models and drug development.

#### ACKNOWLEDGEMENTS

This work was supported by grants from National Key R&D Program of China (2017YFA0103700 and 2016YFC1301204 to HTY), National Natural Science Foundation of China (81520108004, 81470422 to HTY), the Strategic Priority Research Program of the CAS (No. XDA16010201 to HTY), Shanghai Natural Science Foundation (17ZR1435500 to JJH), and the Shenzhen Basic Research Foundation (KQJSCX20170330155020267). The authors thank WiCell Research Institute for providing the H7 hESCs, Dr. Hua-jun Bai (Shanghai Institute of Nutrition and Health) for the assistance in hESC culture, and Prof. Ping Liang from Zhejiang University for the constructive discussion and suggestions.

#### AUTHOR CONTRIBUTIONS

HTY and PZ contributed to the concept and experiment design; PZ, JJH, HL and YJW contributed to the data collection; PZ, HTY, KFOY and MLL contributed to the data analysis; HTY and PZ contributed to the data interpretation and manuscript writing; HTY approved the manuscript and provided the funding support.

#### ADDITIONAL INFORMATION

The online version of this article (<https://doi.org/10.1038/s41401-020-00528-w>) contains supplementary material, which is available to authorized users.

**Competing interests:** The authors declare no competing interests.

#### REFERENCES

1. Clapham DE. Calcium signaling. *Cell*. 2007;131:1047–58.

2. Carafoli E, Krebs J. Why Calcium? How calcium became the best communicator. *J Biol Chem.* 2016;291:20849–57.
3. Slusarski DC, Pelegri F. Calcium signaling in vertebrate embryonic patterning and morphogenesis. *Dev Biol.* 2007;307:1–13.
4. Webb SE, Miller AL. Calcium signalling during embryonic development. *Nat Rev Mol Cell Biol.* 2003;4:539–51.
5. Fearnley CJ, Roderick HL, Bootman MD. Calcium signaling in cardiac myocytes. *Cold Spring Harb Perspect Biol.* 2011;3:a004242.
6. Marks AR. Calcium and the heart: a question of life and death. *J Clin Invest.* 2003;111:597–600.
7. Lan F, Lee AS, Liang P, Sanchez-Freire V, Nguyen PK, Wang L, et al. Abnormal calcium handling properties underlie familial hypertrophic cardiomyopathy pathology in patient-specific induced pluripotent stem cells. *Cell Stem Cell.* 2013;12:101–13.
8. Spater D, Hansson EM, Zangi L, Chien KR. How to make a cardiomyocyte. *Development.* 2014;141:4418–31.
9. He JQ, Ma Y, Lee Y, Thomson JA, Kamp TJ. Human embryonic stem cells develop into multiple types of cardiac myocytes: action potential characterization. *Circ Res.* 2003;93:32–9.
10. Kehat I, Kenyagin-Karsenti D, Snir M, Segev H, Amit M, Gepstein A, et al. Human embryonic stem cells can differentiate into myocytes with structural and functional properties of cardiomyocytes. *J Clin Invest.* 2001;108:407–14.
11. Ma Z, Wang J, Loskill P, Huebsch N, Koo S, Svedlund FL, et al. Self-organizing human cardiac microchambers mediated by geometric confinement. *Nat Commun.* 2015;6:7413.
12. Lee J, Shao NY, Paik DT, Wu H, Guo H, Termglinchan V, et al. SETD7 drives cardiac lineage commitment through stage-specific transcriptional activation. *Cell Stem Cell.* 2018;22:428–44.e5.
13. Liang P, Lan F, Lee AS, Gong T, Sanchez-Freire V, Wang Y, et al. Drug screening using a library of human induced pluripotent stem cell-derived cardiomyocytes reveals disease-specific patterns of cardiotoxicity. *Circulation.* 2013;127:1677–91.
14. Wang J, Liu M, Wu Q, Li Q, Gao L, Jiang Y, et al. Human embryonic stem cell-derived cardiovascular progenitors repair infarcted hearts through modulation of macrophages via activation of signal transducer and activator of transcription 6. *Antioxid Redox Signal.* 2019;31:369–86.
15. Zhu K, Wu Q, Ni C, Zhang P, Zhong Z, Wu Y, et al. Lack of remuscularization following transplantation of human embryonic stem cell-derived cardiovascular progenitor cells in infarcted nonhuman primates. *Circ Res.* 2018;122:958–69.
16. Fu JD, Li J, Tweedie D, Yu HM, Chen L, Wang R, et al. Crucial role of the sarcoplasmic reticulum in the developmental regulation of Ca<sup>2+</sup> transients and contraction in cardiomyocytes derived from embryonic stem cells. *FASEB J.* 2006;20:181–3.
17. Fu JD, Yang HT. Developmental regulation of intracellular calcium homeostasis in early cardiac myocytes. *Sheng Li Xue Bao.* 2006;58:95–103.
18. Guo A, Yang HT. Ca<sup>2+</sup> removal mechanisms in mouse embryonic stem cell-derived cardiomyocytes. *Am J Physiol Cell Physiol.* 2009;297:C732–41.
19. Lam AK, Galione A. The endoplasmic reticulum and junctional membrane communication during calcium signaling. *Biochim Biophys Acta.* 2013;1833:2542–59.
20. Yang HT, Tweedie D, Wang S, Guia A, Vinogradova T, Bogdanov K, et al. The ryanodine receptor modulates the spontaneous beating rate of cardiomyocytes during development. *Proc Natl Acad Sci USA.* 2002;99:9225–30.
21. Yanagida E, Shoji S, Hirayama Y, Yoshikawa F, Otsu K, Uematsu H, et al. Functional expression of Ca<sup>2+</sup> signaling pathways in mouse embryonic stem cells. *Cell Calcium.* 2004;36:135–46.
22. Huang JJ, Wang YJ, Zhang M, Zhang P, Liang H, Bai HJ, et al. Functional expression of the Ca(2+) signaling machinery in human embryonic stem cells. *Acta Pharmacol Sin.* 2017;38:1663–72.
23. Liang J, Wang YJ, Tang Y, Cao N, Wang J, Yang HT. Type 3 inositol 1,4,5-trisphosphate receptor negatively regulates apoptosis during mouse embryonic stem cell differentiation. *Cell Death Differ.* 2010;17:1141–54.
24. Uchida K, Aramaki M, Nakazawa M, Yamagishi C, Makino S, Fukuda K, et al. Gene knock-outs of inositol 1,4,5-trisphosphate receptors types 1 and 2 result in perturbation of cardiogenesis. *PLoS One.* 2010;5:e12500.
25. Mikoshiba K. Role of IP receptor in development. *Cell Calcium.* 2011;49:331–40.
26. Wang YJ, Huang J, Liu W, Kou X, Tang H, Wang H, et al. IP3R-mediated Ca<sup>2+</sup> signals govern hematopoietic and cardiac divergence of Flk1<sup>+</sup> cells via the calcineurin-NFATc3-Etv2 pathway. *J Mol Cell Biol.* 2017;9:274–88.
27. Perez PJ, Ramos-Franco J, Fill M, Mignery GA. Identification and functional reconstitution of the type 2 inositol 1,4,5-trisphosphate receptor from ventricular cardiac myocytes. *J Biol Chem.* 1997;272:23961–9.
28. Lipp P, Laine M, Tovey SC, Burrell KM, Berridge MJ, Li W, et al. Functional InsP<sub>3</sub> receptors that may modulate excitation-contraction coupling in the heart. *Curr Biol.* 2000;10:939–42.
29. Domeier TL, Zima AV, Maxwell JT, Huke S, Mignery GA, Blatter LA. IP<sub>3</sub> receptor-dependent Ca<sup>2+</sup> release modulates excitation-contraction coupling in rabbit ventricular myocytes. *Am J Physiol Heart Circ Physiol.* 2008;294:H596–604.
30. Ju YK, Liu J, Lee BH, Lai D, Woodcock EA, Lei M, et al. Distribution and functional role of inositol 1,4,5-trisphosphate receptors in mouse sinoatrial node. *Circ Res.* 2011;109:848–57.
31. Cooley N, Ouyang K, McMullen JR, Kiriazis H, Sheikh F, Wu W, et al. No contribution of IP<sub>3</sub>R2 to disease phenotype in models of dilated cardiomyopathy or pressure overload hypertrophy. *Circ Heart Fail.* 2013;6:318–25.
32. Li X, Zima AV, Sheikh F, Blatter LA, Chen J. Endothelin-1-induced arrhythmogenic Ca<sup>2+</sup> signaling is abolished in atrial myocytes of inositol-1,4,5-trisphosphate(IP<sub>3</sub>)-receptor type 2-deficient mice. *Circ Res.* 2005;96:1274–81.
33. Signore S, Sorrentino A, Ferreira-Martins J, Kannappan R, Shafaie M, Del Ben F, et al. Inositol 1, 4, 5-trisphosphate receptors and human left ventricular myocytes. *Circulation.* 2013;128:1286–97.
34. Higazi DR, Fearnley CJ, Drawnel FM, Talasila A, Corps EM, Ritter O, et al. Endothelin-1-stimulated InsP<sub>3</sub>-induced Ca<sup>2+</sup> release is a nexus for hypertrophic signaling in cardiac myocytes. *Mol Cell.* 2009;33:472–82.
35. Nakayama H, Bodi I, Maillet M, DeSantiago J, Domeier TL, Mikoshiba K, et al. The IP<sub>3</sub> receptor regulates cardiac hypertrophy in response to select stimuli. *Circ Res.* 2010;107:659–66.
36. Tompkins JD, Jung M, Chen CY, Lin Z, Ye J, Godatha S, et al. Mapping human pluripotent-to-cardiomyocyte differentiation: methylomes, transcriptomes, and exon DNA methylation “memories”. *EBioMedicine.* 2016;4:74–85.
37. Huang J, Zhang M, Zhang P, Liang H, Ouyang K, Yang HT. Coupling switch of P2Y-IP<sub>3</sub> receptors mediates differential Ca<sup>2+</sup> signaling in human embryonic stem cells and derived cardiovascular progenitor cells. *Purinergic Signal.* 2016;12:465–78.
38. Soh BS, Ng SY, Wu H, Buac K, Park JH, Lian X, et al. Endothelin-1 supports clonal derivation and expansion of cardiovascular progenitors derived from human embryonic stem cells. *Nat Commun.* 2016;7:10774.
39. Mazzuca MQ, Khalil RA. Vascular endothelin receptor type B: structure, function and dysregulation in vascular disease. *Biochem Pharmacol.* 2012;84:147–62.
40. Deliu E, Brailoiu GC, Mallilankaraman K, Wang H, Madesh M, Uldieh AS, et al. Intracellular endothelin type B receptor-driven Ca<sup>2+</sup> signal elicits nitric oxide production in endothelial cells. *J Biol Chem.* 2012;287:41023–31.
41. Cao N, Liang H, Yang HT. Generation, expansion, and differentiation of cardiovascular progenitor cells from human pluripotent stem cells. *Methods Mol Biol.* 2015;1212:113–25.
42. Bai HJ, Zhang P, Ma L, Liang H, Wei G, Yang HT. SMYD2 drives mesendodermal differentiation of human embryonic stem cells through mediating the transcriptional activation of key mesendodermal genes. *Stem Cells.* 2019;37:1401–15.
43. Lian X, Hsiao C, Wilson G, Zhu K, Hazeltine LB, Azarin SM, et al. Robust cardiomyocyte differentiation from human pluripotent stem cells via temporal modulation of canonical Wnt signaling. *Proc Natl Acad Sci USA.* 2012;109:E1848–57.
44. Burrifone PW, Matsa E, Shukla P, Lin ZC, Churko JM, Ebert AD, et al. Chemically defined generation of human cardiomyocytes. *Nat Methods.* 2014;11:855–60.
45. Cao N, Liang H, Huang J, Wang J, Chen Y, Chen Z, et al. Highly efficient induction and long-term maintenance of multipotent cardiovascular progenitors from human pluripotent stem cells under defined conditions. *Cell Res.* 2013;23:1119–32.
46. Ouyang K, Leandro Gomez-Amaro R, Stachura DL, Tang H, Peng X, Fang X, et al. Loss of IP3R-dependent Ca<sup>2+</sup> signalling in thymocytes leads to aberrant development and acute lymphoblastic leukemia. *Nat Commun.* 2014;5:4814.
47. Fu X, Toh WS, Liu H, Lu K, Li M, Cao T. Establishment of clinically compliant human embryonic stem cells in an autologous feeder-free system. *Tissue Eng Part C Methods.* 2011;17:927–37.
48. Poon EN, Luo XL, Webb SE, Yan B, Zhao R, Wu SCM, et al. The cell surface marker CD36 selectively identifies matured, mitochondria-rich hPSC-cardiomyocytes. *Cell Res.* 2020;30:626–9.
49. Fu JD, Yu HM, Wang R, Liang J, Yang HT. Developmental regulation of intracellular calcium transients during cardiomyocyte differentiation of mouse embryonic stem cells. *Acta Pharmacol Sin.* 2006;27:901–10.
50. Manfredi O, Maltsev VA, Lakatta EG. Modern concepts concerning the origin of the heartbeat. *Physiology (Bethesda).* 2013;28:74–92.
51. O’Connell TD, Jensen BC, Baker AJ, Simpson PC. Cardiac alpha1-adrenergic receptors: novel aspects of expression, signaling mechanisms, physiologic function, and clinical importance. *Pharmacol Rev.* 2014;66:308–33.
52. Kohi M, Yang HT, Endoh M. Myocardial alpha 1A-adrenoceptor subtypes in rabbit: differentiation by a selective antagonist, HV723. *Eur J Pharmacol.* 1993;250:95–101.
53. Satin J, Itzhaki I, Rapoport S, Schroder EA, Izu L, Arbel G, et al. Calcium handling in human embryonic stem cell-derived cardiomyocytes. *Stem Cells.* 2008;26:1961–72.

54. Resende RR, Adhikari A, da Costa JL, Lorencon E, Ladeira MS, Guatimosim S, et al. Influence of spontaneous calcium events on cell-cycle progression in embryonal carcinoma and adult stem cells. *Biochim Biophys Acta*. 2010;1803:246–60.
55. Garcia MI, Boehning D. Cardiac inositol 1,4,5-trisphosphate receptors. *Biochim Biophys Acta Mol Cell Res*. 2017;1864:907–14.
56. Berridge MJ, Bootman MD, Lipp P. Calcium—a life and death signal. *Nature*. 1998;395:645–8.
57. Luo M, Anderson ME. Mechanisms of altered Ca<sup>2+</sup> handling in heart failure. *Circ Res*. 2013;113:690–708.
58. Yang F, Huang L, Tso A, Wang H, Cui L, Lin L, et al. Inositol 1,4,5-trisphosphate receptors are essential for fetal-maternal connection and embryo viability. *PLoS Genet*. 2020;16:e1008739.
59. Wobus AM, Wallukat G, Hescheler J. Pluripotent mouse embryonic stem cells are able to differentiate into cardiomyocytes expressing chronotropic responses to adrenergic and cholinergic agents and Ca<sup>2+</sup> channel blockers. *Differentiation*. 1991;48:173–82.
60. Lorenzen-Schmidt I, Schmid-Schonbein GW, Giles WR, McCulloch AD, Chien S, Omens JH. Chronotropic response of cultured neonatal rat ventricular myocytes to short-term fluid shear. *Cell Biochem Biophys*. 2006;46:113–22.
61. Xiang Y, Rybin VO, Steinberg SF, Kobilka B. Caveolar localization dictates physiologic signaling of beta 2-adrenoceptors in neonatal cardiac myocytes. *J Biol Chem*. 2002;277:34280–6.
62. Kamp TJ, Hell JW. Regulation of cardiac L-type calcium channels by protein kinase A and protein kinase C. *Circ Res*. 2000;87:1095–102.
63. van der Heyden MA, Wijnhoven TJ, Ophhof T. Molecular aspects of adrenergic modulation of cardiac L-type Ca<sup>2+</sup> channels. *Cardiovasc Res*. 2005;65:28–39.
64. Liu QY, Karpinski E, Pang PK. Changes in alpha 1-adrenoceptor coupling to Ca<sup>2+</sup> channels during development in rat heart. *FEBS Lett*. 1994;338:234–8.
65. Itzhaki I, Rapoport S, Huber I, Mizrahi I, Zwi-Dantsis L, Arbel G, et al. Calcium handling in human induced pluripotent stem cell derived cardiomyocytes. *PLoS One*. 2011;6:e18037.
66. Hund TJ, Ziman AP, Lederer WJ, Mohler PJ. The cardiac IP<sub>3</sub> receptor: uncovering the role of “the other” calcium-release channel. *J Mol Cell Cardiol*. 2008;45:159–61.
67. Hirose M, Stuyvers B, Dun W, Ter Keurs H, Boyden PA. Wide long lasting perinuclear Ca<sup>2+</sup> release events generated by an interaction between ryanodine and IP<sub>3</sub> receptors in canine Purkinje cells. *J Mol Cell Cardiol*. 2008;45:176–84.
68. Prakriya M, Lewis RS. Potentiation and inhibition of Ca<sup>2+</sup> release-activated Ca<sup>2+</sup> channels by 2-aminoethyl-diphenyl borate (2-APB) occurs independently of IP<sub>3</sub> receptors. *J Physiol*. 2001;536:3–19.
69. Mummery C, Ward-van Oostwaard D, Doevendans P, Spijker R, van den Brink S, Hassink R, et al. Differentiation of human embryonic stem cells to cardiomyocytes: role of coculture with visceral endoderm-like cells. *Circulation*. 2003;107:2733–40.
70. Goldberg AT, Bond BR, Mukherjee R, New RB, Zellner JL, Crawford FA Jr, et al. Endothelin receptor pathway in human left ventricular myocytes: relation to contractility. *Ann Thorac Surg*. 2000;69:711–5. discussion 716.
71. Milano CA, Dolber PC, Rockman HA, Bond RA, Venable ME, Allen LF, et al. Myocardial expression of a constitutively active alpha 1B-adrenergic receptor in transgenic mice induces cardiac hypertrophy. *Proc Natl Acad Sci USA*. 1994;91:10109–13.